A numerical study of fully developed laminar flow and heat transfer in a curved pipe with arbitrary curvature ratio

Ru Yang and Sung Fa Chang
Institute of Mechanical Engineering, National Sun Yat-Sen University, Kaohsiung, Taiwan, Republic of China

A finite-difference numerical method is applied to solve the full Navier–Stokes equations for the fully developed flow and heat transfer in an axially uniformly heated curved pipe with arbitrary curvature ratio (the ratio of the pipe radius to the pipe curvature). Previous studies were restricted to within a range of the curvature ratio less than 0.3. In this study, the ranges of the parameters are the curvature ratio varying from 0.01 to 0.9, the Reynolds number varying from 1 to 2,000, and the Prandtl number varying from 0.7 to 300. The results of the friction ratio and the Nusselt-number ratio are correlated with the parameters of the curvature ratio, the Dean number, and the Prandtl number.

Keywords: curved pipe; Dean number; arbitrary curvature ratio

Introduction

Flow in a curved pipe has been extensively studied both theoretically and experimentally. Studies conducted up to 1982 were very well reviewed by Berger, Talbot, and Yao (1983). Most of these were restricted to the case with very small curvature ratio, δ, in which the flow depends only on a single parameter, the Dean number, which indicates the ratio of the centrifugal force to the viscous force. Dean (1927) was one of the first researchers in this area. He employed a perturbation technique to analyze the secondary flow in a curved pipe. Seban and McLaughlin (1963) presented experimental data on friction and heat transfer for the laminar flow of oil and the turbulent flow of water in curved pipes. Mori and Nakayama (1965) solved the governing equations by integral methods, subdividing the flow pattern into a core and a boundary-layer region. Akiyama and Cheng (1971) predicted the fully developed flow and heat transfer characteristics by the boundary vorticity method. Patankar, Pratap, and Spalding (1974) predicted the flow and heat transfer in the developing and developed regions. Prusa and Yao (1982) accounted for the combined effects of both buoyancy and centrifugal force in heated curved tubes. However, in many applications, the value of δ is not very small, and so the aforementioned solutions for $O(\delta) \ll 1$ may not be applicable. Truesdell and Adler (1970) produced a numerical solution of fully developed laminar flow in helically coiled tubes with δ from 0.01 to 0.1. Larrain and Bonilla (1970) presented a serious solution of pressure drop in the laminar flow of fluid in a coiled pipe for κ from 1 to 16 and δ from 0.01 to 0.2. Kalb and Seader (1972) showed that the curvature ratio δ, in the range of 0.01 to 0.1, has a small effect on the peripheral variation of local transport coefficients, but has a negligible influence on the average Nusselt number. Austin and Seader (1973) numerically solved for the Navier–Stokes equations in the vorticity-stream function form for the flow within a rigorously treated toroidal geometry without the assumption of small δ. They reported the solutions up to $\delta = 0.2$. Lee, Simon, and Chow (1985) numerically studied fully developed laminar curved pipe flows and extended δ up to 0.25. Recently, Soh and Berger (1987) reported the solutions of the full Navier–Stokes equation for arbitrary values of δ and presented solutions up to $\delta = 0.2$. The most exhaustive review for the problem was recently given by Kakac, Shah, and Aung (1987). However, the flow in a curved pipe with δ higher than 0.3 has still not been reported. Since the curvature of the pipe can significantly enhance heat transfer and mass transfer rates, curved pipe flow is widely employed in industrial heat exchangers, chemical reactors, and many other devices. In some cases, a greater δ may be considered in industrial design. In addition, blood flow in the human arterial system involving the highly curved aorta has been of particular interest in recent years (Pedley 1980). Therefore, the aim of this study is to extend the work of Austin and Seader (1973) and Soh and Berger (1987) by increasing δ up to 0.9. Of special interest in this study is heat transfer for the curved pipe flow of arbitrary curvature ratio.

Mathematical formulation

The physical problem considered in this study is a fully developed laminar flow in an axially uniformly heated curved pipe. Consequently, the pressure and the temperature gradients are constants along the direction of the main flow, with buoyancy effects omitted. The suitable coordinate system for describing the problem is a curvilinear coordinate system (r', ϕ', θ'), shown in Figure 1. The wall temperature is considered constant on a cross-sectional surface but variable along the axial (θ') direction. The governing equations are

$$\Delta \cdot V = 0$$

$$(V \cdot \nabla)V = -\frac{1}{\rho} \nabla P + \nu \nabla^2 V$$

$$(V \cdot \nabla)T = \alpha \nabla^2 T \qquad (1)$$

Address reprint requests to Professor Yang at the Institute of Mechanical Engineering, National Sun Yat-Sen University, Kaohsiung, Taiwan, Republic of China.

Received 15 December 1991; accepted 14 July 1992

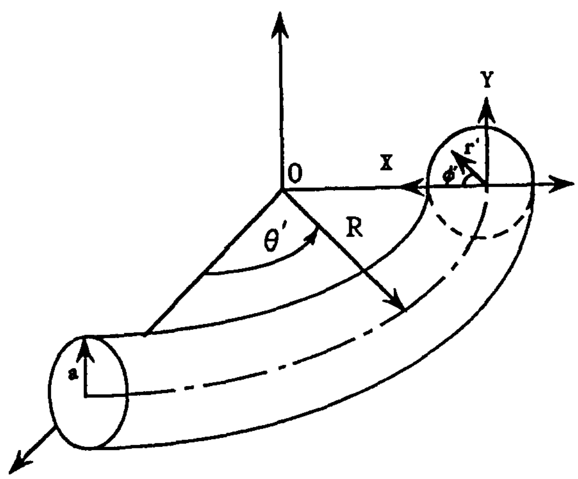

Figure 1 The physical coordinate system

where (u', v', w') are velocity components with respect to (r', ϕ', θ') coordinates. The boundary conditions are the nonslip and the constant-temperature conditions on the wall. The constant pressure gradient G and the constant temperature τ gradient are defined, respectively, as

$$G = -\frac{1}{R}\frac{\partial P'}{\partial \theta'}, \qquad \tau = \frac{1}{R}\frac{\partial T}{\partial \theta'} \tag{2}$$

In order to nondimensionalize the above equations, the following dimensionless variables are defined:

$$\delta = \frac{a}{R}, r = \frac{r'}{a}, \phi = \phi', \theta = \frac{\theta'}{\sqrt{\delta}}, W_0 = \frac{Ga^2}{4\mu}, w = \frac{w'}{W_0}, u = \frac{u'}{\sqrt{\delta}W_0}$$

$$v = \frac{v'}{\sqrt{\delta}W_0}, \mathrm{Re}_s = \frac{W_0 a}{\nu}, \mathrm{De} = \delta\,\mathrm{Re}_s^2, H = \frac{T_w - T}{\tau a} \tag{3}$$

where W_0 represent the maximum velocity for a fully developed flow in a straight pipe with the pressure gradient G, and δ, Re_s, and De are the curvature ratio, the Reynolds number, and the Dean number, respectively. The dimensionless governing equations for the fully developed flow become

$$\frac{\partial}{\partial r}[(1 - \delta r\cos\phi)ru] + \frac{\partial}{\partial \phi}[(1 - \delta r\cos\phi)v] = 0 \tag{4}$$

$$u\frac{\partial u}{\partial r} + \frac{v}{r}\frac{\partial u}{\partial \phi} - \frac{v^2}{r} + \frac{w^2\cos\phi}{1 - \delta r\cos\phi} = -\frac{1}{\delta}\frac{\partial p}{\partial r} - \frac{1}{\sqrt{\mathrm{De}}}\left[\left(\frac{1}{r}\frac{\partial}{\partial \phi} + \frac{\delta\sin\phi}{1 - \delta r\cos\phi}\right)\left(\frac{v}{r} + \frac{\partial v}{\partial r} - \frac{1}{r}\frac{\partial u}{\partial \phi}\right)\right] \tag{5}$$

$$u\frac{\partial v}{\partial r} + \frac{v}{r}\frac{\partial v}{\partial \phi} + \frac{uv}{r} - \frac{w^2\sin\phi}{1 - \delta r\cos\phi} = -\frac{1}{\delta r}\frac{\partial p}{\partial \phi} + \frac{1}{\sqrt{\mathrm{De}}}\left[\left(\frac{\partial}{\partial r} - \frac{\delta\cos\phi}{1 - \delta r\cos\phi}\right)\left(\frac{v}{r} + \frac{\partial v}{\partial r} - \frac{1}{r}\frac{\partial u}{\partial \phi}\right)\right] \tag{6}$$

Notation

a	Pipe radius
De	Dean number, $\delta\mathrm{Re}_s^2$
f	Dimensionless stream function
F_c	Friction factor of curved pipe
F_s	Friction factor of straight pipe
G	Axial pressure gradient, $-\frac{1}{R}\frac{\partial P'}{\partial \theta'}$
H	$\frac{T_w - T}{\tau a}$
h	Heat transfer coefficient
$\bar{h}$	Mean heat transfer coefficient
k	Thermal conductivity
Nu	Nusselt number
P	$\frac{P'}{\rho W_0^2}$
P'	Dimensional pressure
Q	Volumetric flow rate
R	Radius of curvature
Re_c	Curved pipe Reynolds number, $\frac{w'_m 2a}{\nu}$
Re_s	Straight pipe Reynolds number, $\frac{W_0 a}{\nu}$
T	Temperature
T_w	Wall temperature
T_0	Reference temperature
u	$\frac{u'}{\sqrt{\delta}W_0}$
u'	Dimensional velocity in r' direction
v	$\frac{v'}{\sqrt{\delta}W_0}$
v'	Dimensional velocity in ϕ' direction
w	$\frac{w'}{W_0}$
w'	Dimensional velocity in θ' direction
W_0	Centerline velocity of developed flow in a straight pipe with pressure gradient G, $\frac{Ga^2}{4\mu}$

Greek symbols

α	Thermal diffusivity
δ	Curvature ratio, $\frac{a}{R}$
κ	$\frac{2aw'_m}{\nu}\left(\frac{a}{R}\right)^{1/2}$
μ	Dynamic viscosity
ν	Kinematic viscosity
ρ	Fluid density
τ	Axial temperature gradient, $\frac{1}{R}\frac{\partial T}{\partial \theta'}$

Subscripts

c	Quantities associated with the curved pipe
m	Mixed mean value
s	Quantities associated with the straight pipe

$$u\frac{\partial w}{\partial r}+\frac{v}{r}\frac{\partial w}{\partial \phi}-\frac{\delta w}{1-\delta r\cos\phi}(v\sin\phi-u\cos\phi)=\frac{1}{1-\delta r\cos\phi}\frac{4}{\sqrt{\mathrm{De}}}+\frac{1}{\sqrt{\mathrm{De}}}\left[\frac{1}{r}\frac{\partial}{\partial\phi}\left(\frac{1}{r}\frac{\partial w}{\partial\phi}+\frac{w\delta\sin\phi}{1-\partial r\cos\phi}\right)+\left(\frac{1}{r}+\frac{\partial}{\partial r}\right)\left(\frac{\partial w}{\partial r}-\frac{w\delta\cos\phi}{1-\delta r\cos\phi}\right)\right] \tag{7}$$

$$u\frac{\partial H}{\partial r}+\frac{v}{r}\frac{\partial H}{\partial\phi}-\frac{1}{\sqrt{\delta}}\frac{w}{1-\delta r\cos\phi}=\frac{1}{\mathrm{Pr}\sqrt{\mathrm{De}}}\frac{1}{1-\delta r\cos\phi}\left[(1-\delta r\cos\phi)\frac{\partial^2 H}{\partial r^2}+(1-2\delta r\cos\phi)\frac{1}{r}\frac{\partial H}{\partial r}+(1-\delta r\cos\phi)\frac{1}{r^2}\frac{\partial^2 H}{\partial\phi^2}+\frac{\delta\sin\phi}{r}\frac{\partial H}{\partial\phi}\right] \tag{8}$$

and the boundary conditions become

$$u=v=w=H=0 \quad \text{at } r=1 \tag{9}$$

A stream function can be defined to satisfy Equation 4 as

$$u=\frac{1}{r(1-\delta r\cos\phi)}\frac{\partial f}{\partial\phi},\quad v=-\frac{1}{1-\delta r\cos\phi}\frac{\partial f}{\partial r} \tag{10}$$

and the dimensionless vorticity in the θ direction is defined by

$$\omega=\frac{v}{r}+\frac{\partial v}{\partial r}-\frac{1}{r}\frac{\partial u}{\partial\phi} \tag{11}$$

Then, by substituting f and ω into Equations 4 to 9 and eliminating the pressure terms in the u and v momentum equations, one ends up with the following equations:

$$\left[\left(\frac{\partial^2 f}{\partial r^2}+\frac{1}{r}\frac{\partial f}{\partial r}+\frac{1}{r}\frac{\partial^2 f}{\partial\phi^2}\right)-\frac{1}{r(1-\delta r\cos\phi)}\left(\sin\phi\frac{\partial f}{\partial\phi}-r\cos\phi\frac{\partial f}{\partial r}\right)\right]+(1-\partial r\cos\phi)\omega=0 \tag{12}$$

$$\left(\frac{\partial f}{\partial r}\frac{\partial\omega}{\partial\phi}-\frac{\partial f}{\partial\phi}\frac{\partial\omega}{\partial r}\right)+\omega\left(\frac{\partial^2 f}{\partial r\partial\phi}-\frac{\delta r\sin\phi}{1-\delta r\cos\phi}\frac{\partial f}{\partial r}\right)+\frac{1}{r(1-\delta r\cos\phi)}\left(\frac{\partial^2 f}{\partial r\,\partial\phi}-\frac{\delta\cos\phi}{1-\delta r\cos\phi}\frac{\partial f}{\partial\phi}\right)\times\left(\frac{1}{r}\frac{\partial^2 f}{\partial\phi^2}-\frac{\delta\sin\phi}{1-\delta r\cos\phi}\frac{\partial f}{\partial\phi}+\frac{1}{1-\delta r\cos\phi}\frac{\partial f}{\partial r}+r\frac{\partial^2 f}{\partial r^2}\right)+2w\left(\cos\phi\frac{\partial w}{\partial\phi}-r\sin\phi\frac{\partial w}{\partial r}\right)=-\frac{1}{\sqrt{\mathrm{De}}}\times\left[r(1-\delta r\cos\phi)\left(\frac{\partial^2\omega}{\partial r^2}+\frac{1}{r}\frac{\partial\omega}{\partial r}+\frac{1}{r}\frac{\partial^2\omega}{\partial\phi^2}\right)+\delta\left(\sin\phi\frac{\partial\omega}{\partial\phi}-r\cos\phi\frac{\partial\omega}{\partial r}\right)-\frac{\delta^2 r\omega}{1-\delta r\cos\phi}\right] \tag{13}$$

$$\left(\frac{\partial f}{\partial\phi}\frac{\partial w}{\partial r}-\frac{\partial f}{\partial r}\frac{\partial w}{\partial\phi}\right)-\frac{\delta w}{1-\delta r\cos\phi}\left(\cos\phi\frac{\partial f}{\partial\phi}+r\sin\phi\frac{\partial w}{\partial r}\right)=\frac{4r}{\sqrt{\mathrm{De}}}+\frac{1}{\sqrt{\mathrm{De}}}\left[r(1-\delta r\cos\phi)\left(\frac{\partial^2 w}{\partial r^2}+\frac{1}{r}\frac{\partial w}{\partial r}+\frac{1}{r}\frac{\partial^2 w}{\partial\phi^2}\right)+\delta\left(\sin\phi\frac{\partial w}{\partial\phi}-r\cos\phi\frac{\partial w}{\partial r}\right)-\frac{\delta^2 rw}{1-\delta r\cos\phi}\right] \tag{14}$$

$$\left(\frac{\partial f}{\partial\phi}\frac{\partial H}{\partial r}-\frac{\partial f}{\partial r}\frac{\partial H}{\partial\phi}\right)-\frac{rw}{\sqrt{\delta}}=\frac{r}{\mathrm{Pr}\sqrt{\mathrm{De}}}\times\left[(1-\delta r\cos\phi)\left(\frac{\partial^2 H}{\partial r^2}+\frac{1}{r}\frac{\partial H}{\partial r}+\frac{1}{r}\frac{\partial^2 H}{\partial\phi^2}\right)-\delta\left(\cos\phi\frac{\partial H}{\partial r}-\frac{\sin\phi}{r}\frac{\partial H}{\partial\phi}\right)\right] \tag{15}$$

Since the problem is symmetrical, only a half domain ($\phi=0°$ to $180°$) must be solved. Therefore, the boundary conditions become

$$r=1\quad f=w=H=0,\ \omega=-\frac{1}{1-\delta r\cos\phi}\frac{\partial^2 f}{\partial r^2} \tag{16}$$

$$\phi=0,\pi\quad f=\omega=\frac{\partial w}{\partial\phi}=\frac{\partial H}{\partial\phi}=0 \tag{17}$$

Since $r=0$ is a singular point in the (r,ϕ,θ) coordinate system, the equations at this point are solved in the x-y coordinate system shown in Figure 1. The equations at this point are

$$\frac{\partial f}{\partial y}\frac{\partial w}{\partial x}-\delta w\frac{\partial f}{\partial y}=\frac{4}{\sqrt{\mathrm{De}}}+\frac{1}{\sqrt{\mathrm{De}}}\left(\frac{\partial^2 w}{\partial x^2}+\frac{\partial^2 w}{\partial y^2}-\delta\frac{\partial w}{\partial x}-\delta^2 w\right) \tag{18}$$

$$\frac{\partial f}{\partial y}\frac{\partial H}{\partial x}-\frac{w}{\sqrt{\delta}}=\frac{1}{\mathrm{Pr}\sqrt{\mathrm{De}}}\left(\frac{\partial^2 H}{\partial x^2}+\frac{\partial^2 H}{\partial y^2}-\delta\frac{\partial H}{\partial x}\right) \tag{19}$$

The parameters presented in the dimensionless governing equations are curvature ratio (δ), Dean number (De), and Prandtl number (Pr). Since the curvature ratio effect is emphasized in this study, it is more convenient to use Reynolds number for a fixed axial pressure gradient, Re_s, instead of De for the data presentation.

The equations are solved numerically via a finite-difference scheme and the Gauss–Seidel iteration method. The grid size of (21, 37) corresponding to (r,ϕ) was considered sufficient after several tests of different grid sizes. The convergence criterion was found to be sufficient when all relative errors of the dependent variables were less than 10^{-4}.

Numerical results and discussion

The results of the flow and the heat transfer are presented in terms of the friction ratio and the dimensionless heat transfer (Nusselt number) ratio, respectively. Following Soh and Berger (1987), the friction ratio is defined as the ratio of the flow rate in a curved pipe to that in a straight pipe for the same pressure gradient, i.e.,

$$\frac{F_c}{F_s}=\frac{Q_s}{Q_c}=\frac{\pi}{4I},\quad I=\int_0^1\int_0^\pi wr\,dr\,d\phi \tag{20}$$

Similarly, the Nusselt number ratio is defined as the ratio of the mean peripheral Nusselt number in a curved pipe to that in a straight pipe for the same temperature gradient, i.e.,

$$\frac{\overline{\mathrm{Nu}}_c}{\overline{\mathrm{Nu}}_s} = \frac{11}{48}\overline{\mathrm{Nu}}_c \tag{21}$$

The mean peripheral Nusselt number is defined by

$$\overline{\mathrm{Nu}}_c = \frac{2ah}{k} = \frac{\int_0^\pi \mathrm{Nu}_c(1 - \delta\cos\phi)d\phi}{\int_0^\pi (1 - \delta\cos\phi)d\phi} \tag{22}$$

where the local Nusselt number is defined as

$$\mathrm{Nu}_c = \frac{2ah}{k} = \frac{-2I(\partial H/\partial r)|_{r=1}}{\int_0^1\int_0^\pi Hwr\,dr\,d\phi} \tag{23}$$

and the heat transfer coefficient is defined as

$$k\left.\frac{\partial T}{\partial r'}\right|_{r'=a} = h(T_w - T_m) \tag{24}$$

The results are first compared with the existing data to ensure that the computational scheme is correct. Table 1 shows the comparison of the friction ratio. The parameter κ in the table is the other form of the Dean number defined in the literature (Austin and Seader 1973; Soh and Berger 1987) as

$$\kappa = \frac{2aw'_m}{\nu}\left(\frac{a}{R}\right)^{1/2} \tag{25}$$

It can be seen that the results agree very well (within 1 percent of error) with the data of other literature. It is worth noting that, for certain small κ, the friction ratio is less than 1. This phenomenon has been reported by Topakoglu (1967), Larrain and Bonilla (1970), and Soh and Berger (1987).

The data for heat transfer are relatively scarce in the literature. Table 2 shows the comparison of the results of this work with those of Austin and Seader (1973). The agreement is within 2.5 percent in relative error.

Results for the velocity field

It is well known that due to the centrifugal force induced by the pipe curvature, a secondary flow forms in a curved pipe flow and the maximum axial velocity departs from the center of the pipe toward the outer bend wall. Since the centrifugal force is proportional to the square of the axial velocity and inversely proportional to the curvature radius of the pipe, increased Re_s and δ both result in increasing the centrifugal force. Besides, the effect of Re_s should be stronger than the effect of δ. Figure 2 shows that the maximum axial velocity has departed further from the center of the pipe when Re_s is increased. This phenomenon holds for the range of Re_s within this study, i.e., $1 < \mathrm{Re}_s < 2000$. On the other hand, Figure 3 illustrates the effect of δ on the position of the maximum axial velocity. It is shown that the maximum axial velocity also departs further from the center of the pipe when δ is increased. However, when δ is increased to a certain value, further increases in δ causes the maximum axial velocity to return closer to the center of the pipe. The reason is that when δ is high, the increased friction loss reduces the axial velocity, which results in decreasing the centrifugal force, and overcoming the effect of δ on increasing the centrifugal force. This phenomenon is shown in Figure 3 when comparing the maximum velocities of the cases of $\delta = 0.01$, 0.1, and 0.4.

Figure 4 shows the effect of Re_s on the secondary flow. It can be seen that the center of the secondary flow is closer to the pipe wall when Re_s is higher. That is, the greater the Re_s, the larger the centrifugal dominant region and the smaller the viscous dominant region. Similar phenomenon can be observed in Figure 5 for the results of varying δ while fixing Re_s.

Results for the temperature field

The effects of Re_s and δ on the temperature profile are similar to those on the axial velocity profile that were discussed

Table 1 The comparison of the friction ratio F_c/F_s

δ	κ	Lorrain & Bonilla (1970)	Austin & Seader (1973)	Soh & Berger (1987)	This work
0.01	0.885			0.9987	0.9999
0.01	1.00	1.000	1.000		1.0000
0.01	4.998	1.0003	1.001		1.0002
0.01	66.15			1.3362	1.3390
0.1	15.343	1.0302			1.0305
0.1	102.33			1.5538	1.5451
0.2	4.463		1.002		1.0006
0.2	88.29			1.5200	1.5196

Table 2 The comparison of the heat transfer ratio $\overline{\mathrm{Nu}}_c/\overline{\mathrm{Nu}}_s$

δ	κ	Pr	Austin & Seader (1973)	This work
0.01	100.3	0.7	1.7875	1.7452
0.1	100.8	0.7	1.7875	1.8136
0.1	10.4	0.7	1.0000	1.0250
0.1	10.4	100	2.0850	2.0513
0.1	10.4	200	2.4060	2.3810

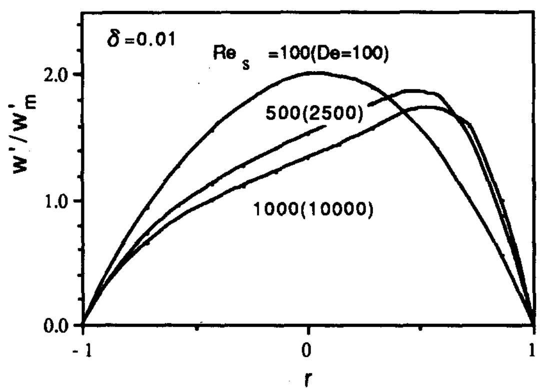

Figure 2 Profiles of axial velocity for various Re_s

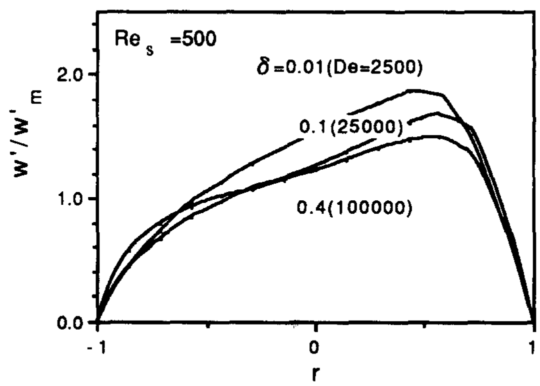

Figure 3 Profiles of axial velocity for various δ

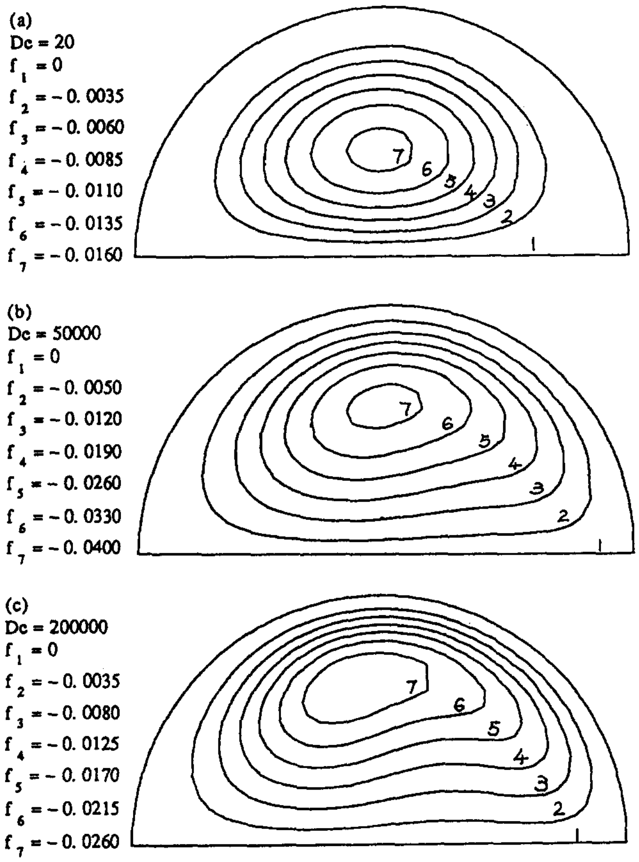

Figure 4 Secondary flow patterns for various Re_s, $\delta = 0.2$

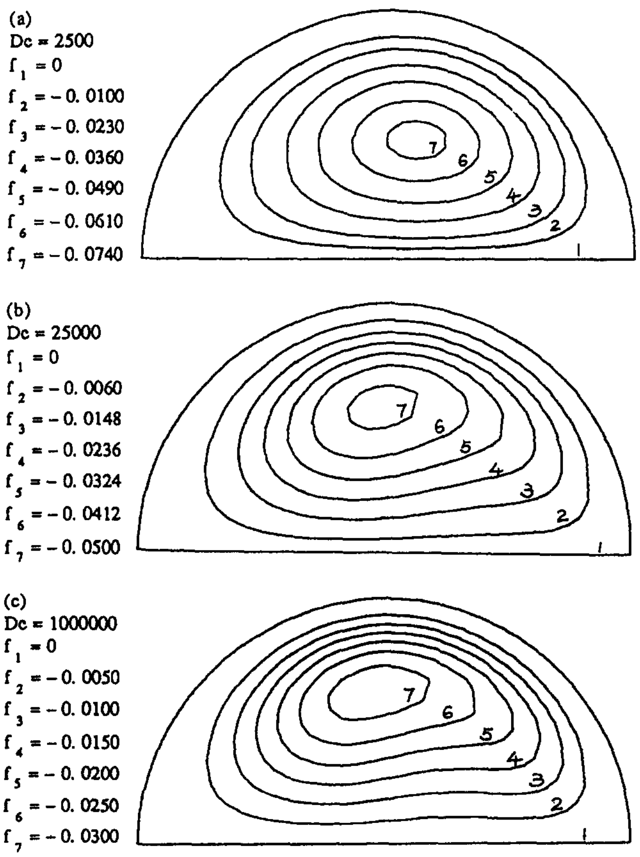

Figure 5 Secondary flow patterns for various δ, $Re_s = 500$

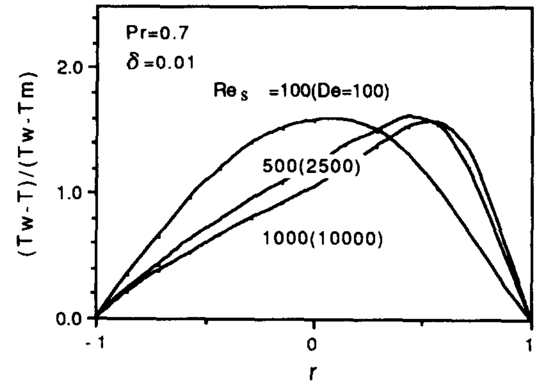

Figure 6 Re_s effect on temperature profile

previously, and are shown in Figures 6 and 7. Figure 8 shows the effect of the Prandtl number (Pr) on the temperature profile. The effect of the Prandtl number is similar to that of Re_s, except that the temperature decreases significantly when Pr increases.

Results for the friction ratio

It is shown in Figure 9 that an increase of Re_s results in an increased friction ratio. For the range of Re_s less than 10, the friction ratio may become less than 1. That is, the friction loss in the curved pipe become less than the friction loss in a straight pipe. This phenomenon has been reported by Topakoglu (1967), Larrain and Bonilla (1970), and Soh and Berger (1987) as mentioned earlier. The effect of δ on the friction ratio is shown in Figure 10. It can be seen that δ has a prominent effect

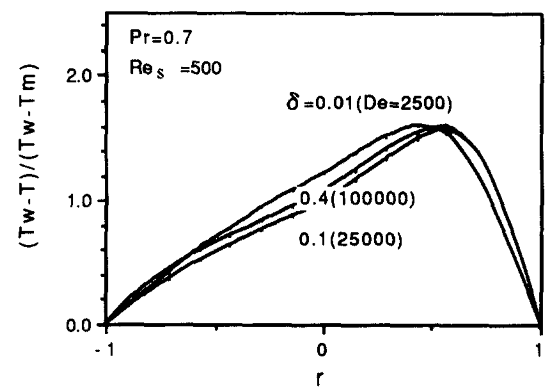

Figure 7 δ effect on temperature profile

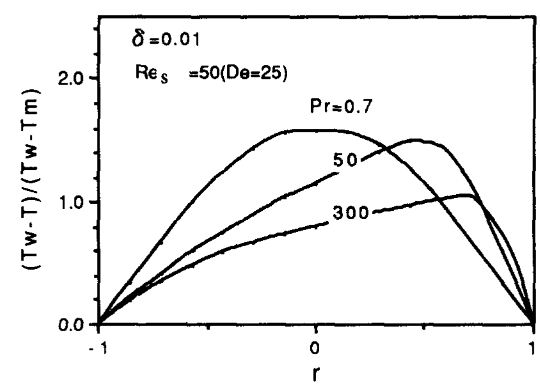

Figure 8 Pr effect on temperature profile

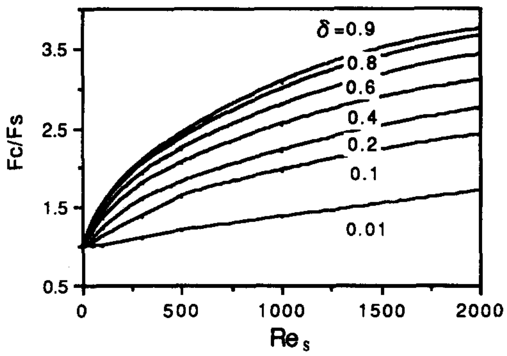

Figure 9 Re_s effect on friction ratio

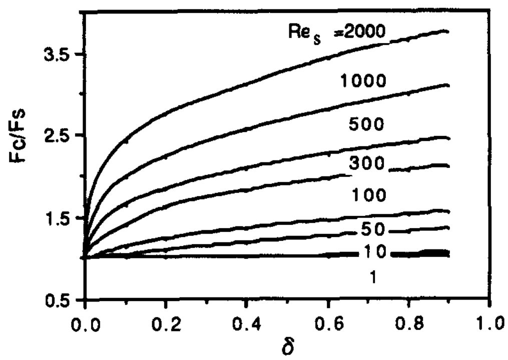

Figure 10 δ effect on friction ratio

on increasing the friction loss except for the range of $Re_s < 10$. Figure 11 shows the friction ratio as the function of De. All the data fall on a single curve, even for a large δ. This suggests that the friction ratio can be correlated by a single parameter, De, for the entire range of the curvature ratio, and the correlations obtained in the previous studies (Kakac et al. 1987) for $\delta < 0.3$ can all be extended to at least $\delta = 0.9$.

Results for the heat transfer ratio

The secondary flow induced by the curvature of the pipe has the normal effect of enhancing heat transfer. When Re_s is increased, the heat transfer rate increases. This is shown in Figure 12 for $Pr = 0.7$ and in Figure 13 for $Pr = 5$. On the other hand, the heat transfer does not necessarily increase with increasing δ. As shown in Figure 14 for $Pr = 0.7$, for a fixed Re_s, the heat transfer rate increases with increasing δ until a certain

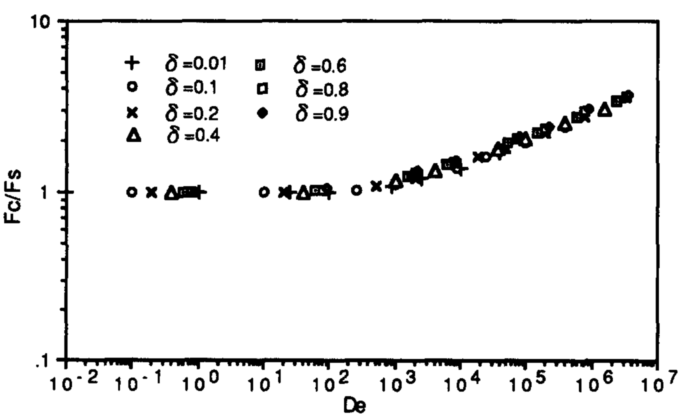

Figure 11 Friction ratio vs. Dean number

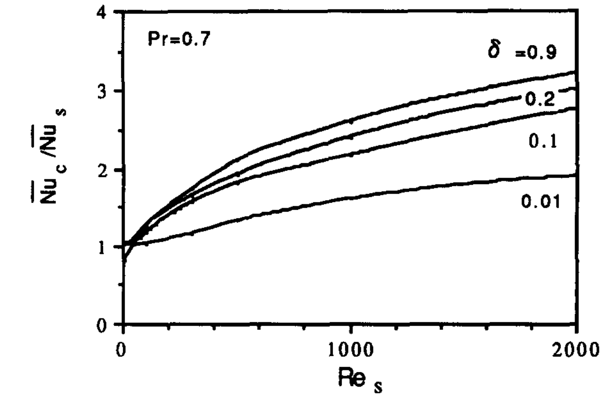

Figure 12 Re_s effect on heat transfer ratio, $Pr = 0.7$

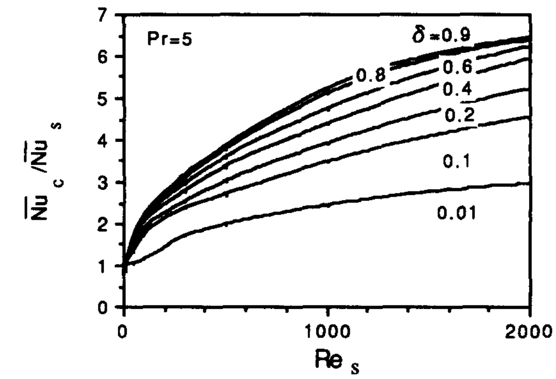

Figure 13 Re_s effect on heat transfer ratio, $Pr = 5$

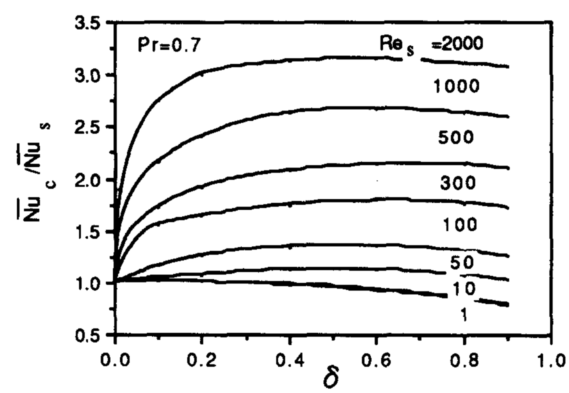

Figure 14 δ effect on heat transfer ratio, $Pr = 0.7$

value of δ; at that point, the heat transfer rate no longer varies significantly with δ and may become slightly decreasing with increasing δ. However, for a very small Re_s, the heat transfer ratio is monotonically decreasing with increasing curvature ratio. This phenomenon also holds for $Pr = 5$. Figure 15 illustrates the results of the curvature ratio effects on the heat transfer ratio for $Pr = 5$. The optimum δ no longer exists for $Re_s > 50$. Therefore, for a given pressure gradient corresponding to $Re_s > 50$ of the flow of water in a curved pipe, the larger the curvature the more the enhancement of the heat transfer.

The Prandtl number's effect on the heat transfer ratio are shown in Figure 16. It can be seen, for the case of $\delta = 0.01$ and $Re_s = 50$, that the higher Prandtl-number fluid flow in a curved pipe results in a higher heat transfer ratio. Figure 17 shows the results of the Prandtl number's effect on the heat transfer ratio for a very small Re_s ($Re_s = 1$). The results illustrate that the

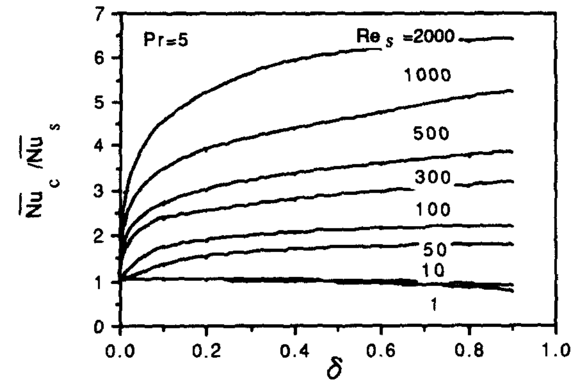

Figure 15 δ effect on heat transfer ratio, Pr = 5

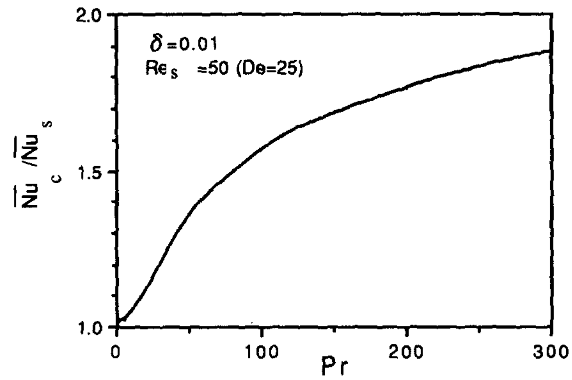

Figure 16 Pr effect on heat transfer ratio

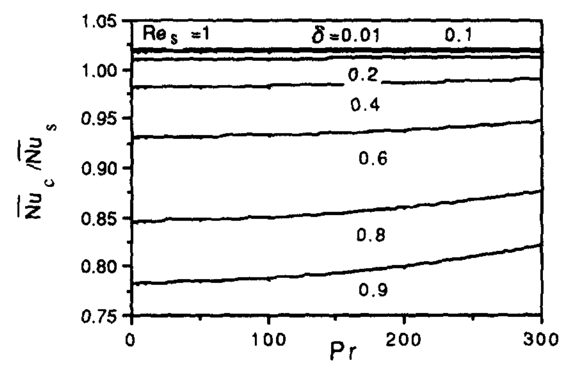

Figure 17 Results of heat transfer ratio for $Re_s = 1$

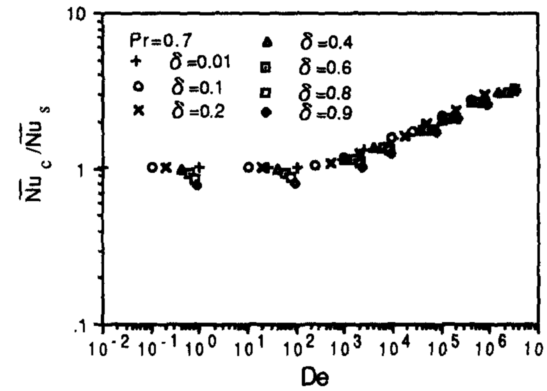

Figure 18 Heat transfer ratio vs. Dean number, Pr = 0.7

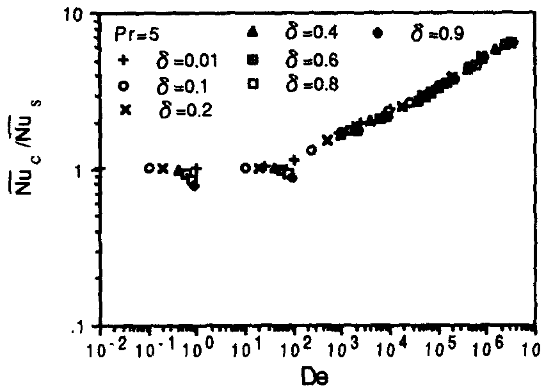

Figure 19 Heat transfer ratio vs. Dean number, Pr = 5

curvature actually depresses the heat transfer for a very small Re_s. The figure also indicates that the depressing effect of heat transfer ratio is more prominent for the smaller Prandtl number. Figures 18 and 19 show the Nusselt number ratio as a function of the Dean number for Pr = 0.7 and 5, respectively. The increased curvature ratio has a prominent effect on decreasing the heat transfer ratio. The reason is that when the curvature ratio is high, the flow rate is much lower in a curved pipe than that in a straight pipe for the same pressure gradient. Therefore, the heat transfer ratio cannot be correlated by the parameters of De and Pr only; instead, it must be correlated by the parameters of De, Pr, and δ.

Conclusions

This paper reports a numerical study of the fully developed flow and heat transfer in a curved pipe with various curvature ratio. The range of the parameters are the curvature ratio varying from 0.01 to 0.9, the Reynolds number varying from 1 to 2,000 and the Prandtl number varying from 0.7 to 300. The results indicate, except for the range of low Re_s ($Re_s < 10$), that the friction ratio increases with increasing pressure gradient and increasing curvature ratio. On the other hand, the heat transfer ratio increases with increasing δ until at a certain value of δ, the heat transfer rate no longer varies significantly with δ. In addition, for very low Re_s (such as $Re_s = 1$), the increasing curvature ratio actually depresses the heat transfer. In this study, however, the buoyancy effect is not considered. This may restrict the applicability of the present results to cases other than those of very low Re_s and very high heat transfer rates. The inclusion of buoyancy effect is a proposed future study.

The present results for the friction ratio and the heat transfer ratio can be correlated with the parameters of the curvature ratio, the Dean number and the Prandtl number. The results are given below.

The friction ratio for $\delta < 0.9$ is

$$\frac{F_c}{F_s} = 1 \qquad \mathrm{De} \le 500$$

$$\frac{F_c}{F_s} = 0.397\,\mathrm{De}^{0.149} \qquad \mathrm{De} > 500 \tag{26}$$

The heat transfer ratio for $0.01 < \delta < 0.9$; $0.7 < \mathrm{Pr} < 5$ and $10^{-2} < \mathrm{De} < 10^{6}$ is

$$\frac{\overline{\mathrm{Nu}}_c}{\overline{\mathrm{Nu}}_s} = 0.722\,\mathrm{De}^{0.098}\delta^{-0.015}\,\mathrm{Pr}^{0.181} \tag{27}$$

Acknowledgment

The authors gratefully acknowledge the financial support of the National Science Council, Taiwan under the contract NSC80-0401-E-110-04 in supporting this research.

References

Akiyama, M. and Cheng, K. C. 1971. Boundary vorticity method for laminar forced convection heat transfer in curved pipes. *Int. J. Heat Mass Transfer*, **14**, 1659–1675

Austin, L. R. and Seader, J. D. 1973. Fully developed viscous flow in coiled circular pipes. *AIChE J.*, **19**, 85–94

Berger, S. A., Talbot, L., and Yao, L. S. 1983. Flow in curved pipe. *Annu. Rev. Fluid Mech.*, **15**, 461–412

Dean, W. R. 1927. Note on the motion of fluid in a curved pipe. *Philos. Mag.*, **20**, 208–223

Kakac, S., Shah, R. A., and Aung, W. 1987. *Handbook of Single-Phase Convective Heat Transfer.* Wiley, New York, Chapter 5

Kalb, C. E. and Seader, J. D. 1972. Heat and mass transfer phenomena for viscous flow in curved circular tubes. *Int. J. Heat Mass Transfer*, **15**, 801–817

Larrain, J. and Bonilla, C. F. 1970. Theoretical analysis of pressure drop in the laminar flow of fluid in a coiled pipe. *Trans. Soc. Rheol.*, **14**, 135–147

Lee, J-B., Simon, H. A., and Chow, J. C. F. 1985. Buoyancy in developed laminar curved tube flows. *Int. J. Heat Mass Transfer*, **28**, 631–640

Mori, Y. and Nakayama, W. 1965. Study on forced convective heat transfer in curved pipes. *Int. J. Heat Mass Transfer*, **8**, 67–82

Patankar, S. V., Pratap, V. S., and Spalding, D. B. 1974. Prediction of laminar flow and heat transfer in helically coiled pipes. *J. Fluid Mech.*, **62**, 539–551

Pedley, T. J. 1980. *The Fluid Mechanics of Large Blood Vessels.* Cambridge University Press, Cambridge, 160–234

Prusa, J. and Yao, L. S. 1982. Numerical solution for fully developed flow in heated curved tubes. *J. Fluid Mech.*, **123**, 503–522

Seban, R. A. and McLaughlin, E. F. 1963. Heat transfer in tube coils with laminar and turbulent flow. *Int. J. Heat Mass Transfer*, **6**, 387–395

Soh, W. Y. and Berger, S. A. 1987. Fully developed flow in a curved pipe of arbitrary curvature ratio. *Int. J. Numer. Meth. Fluids*, **7**, 733–755

Topakoglu, H. C. 1967. Steady laminar flows of an incompressible viscous fluid in curved pipes. *J. Math. Mech.*, **16**, 1321–1328

Truesdell, L. C. and Adler, R. J. 1970. Numerical treatment of fully developed laminar flow in helically coiled tubes. *AIChE J.*, **16**, 1010–1015